Clim. Past, 7, 693–706, 2011
www.clim-past.net/7/693/2011/
doi:10.5194/cp-7-693-2011

Climate of the Past

Boron isotope fractionation during brucite deposition from artificial seawater

J. Xiao[1], Y. K. Xiao[2,3], C. Q. Liu[3], and Z. D. Jin[1]

[1]State Key Laboratory of Loess and Quaternary Geology, Institute of Earth Environment, Chinese Academy of Sciences, Xi'an, 710075, China
[2]Qinghai Institute of Salk Lakes, Chinese Academy of Sciences, Xining, Qinghai, 810008, China
[3]State Key Laboratory of Environmental Geochemistry, Institute of Geochemistry, Chinese Academy of Sciences, Guiyang, 550002, China

Received: 21 February 2011 – Published in Clim. Past Discuss.: 2 March 2011
Revised: 23 May 2011 – Accepted: 6 June 2011 – Published: 6 July 2011

Abstract. Experiments involving boron incorporation into brucite ($Mg(OH)_2$) from magnesium-free artificial seawater with pH values ranging from 9.5 to 13.0 were carried out to better understand the incorporation behavior of boron into brucite and the influence of it on Mg/Ca-SST proxy and δ^{11}B-pH proxy. The results show that both the concentration of boron in deposited brucite ($[B]_d$) and its boron partition coefficient (K_d) between deposited brucite and final seawater are controlled by the pH of the solution. The incorporation capacity of boron into brucite is almost the same as that into corals, but much stronger than that into oxides and clay minerals. The isotopic compositions of boron in deposited brucite ($\delta^{11}B_d$) are higher than those in the associated artificial seawater ($\delta^{11}B_{isw}$) with fractionation factors ranging between 1.0177 and 1.0569, resulting from the preferential incorporation of $B(OH)_3$ into brucite. Both boron adsorptions onto brucite and the precipitation reaction of H_3BO_3 with brucite exist during deposition of brucite from artificial seawater. The simultaneous occurrence of both processes determines the boron concentration and isotopic fractionation of brucite. The isotopic fractionation behaviors and mechanisms of boron incorporated into brucite are different from those into corals. The existence of brucite in corals can affect the δ^{11}B and Mg/Ca in corals and influences the Mg/Ca-SST proxy and δ^{11}B-pH proxy negatively. The relationship between δ^{11}B and Mg/Ca in corals can be used to judge the existence of brucite in corals, which should provide a reliable method for better use of δ^{11}B and Mg/Ca in corals to reconstruct paleo-marine environment.

Correspondence to: Y. K. Xiao
(xiaoyk@isl.ac.cn)

1 Introduction

Mg is a common trace element in corals and the Mg/Ca ratio has been used to investigate the paleothermometry of seawater (Watanabe et al., 2001; Mitsuguchi et al., 2008; Wei et al., 2009; Allison et al., 2010). The incorporation of Mg into coral skeleton is controlled by varying factors. Mg can exist in the form of brucite in corals (Smith and Delong, 1978; Nothdurft et al., 2005) and Mg content in *scleractinian* corals varies between different genera and localities (Fallon et al., 1999). Nothdurft et al. (2005) studied brucite in living *scleractinian* corals colonies (*Acropora*, *Pocillopora*, *Porites*) from subtidal and intertidal settings in the Great Barrier Reef, Australia, and subtidal *Montastraea* from the Florida Keys, United States. Their results suggested that high containing activity combined with high pH and low pCO_2 led to localized brucite precipitation in organic biofilms of coral skeletons and that brucite in living coral skeletons is an indicator of extreme microenvironments in shallow-marine settings. The occurrence of brucite in corals can bring a higher Mg/Ca ratio and be responsible for reported anomalies in Mg/Ca vs. sea-surface temperature (SST) plots in corals (Nothdurft et al., 2005). Defining the source of such anomalies is critical for using Mg/Ca in corals to reconstruct the paleothermometry of seawater (Mg/Ca-SST proxy).

In recent years, topics such as the reconstruction of ancient seawater pH using the isotopic composition of boron in corals, the calculation of the past pCO_2, and the influence of these two factors on changes in the ancient climate, have become important issues for the international boron isotope geochemistry community (δ^{11}B-pH proxy) (Hemming and Hanson, 1992; Gaillardet and Allègre, 1995; Pelejero et al., 2005; Liu et al., 2009; Wei et al., 2009; Douville et al., 2010).

Published by Copernicus Publications on behalf of the European Geosciences Union.

Table 1. Chemical composition of magnesium-free, artificial seawater.

Chemical composition	NaCl	$CaCl_2$	$NaHCO_3$	KCl	NaBr	H_3BO_3	Na_2SiO_3	$Na_2Si_4O_9$	H_3PO_4	Al_2Cl_6	$LiNO_3$
Concentration ($g\,l^{-1}$)	26.7260	1.1530	0.1980	0.7210	0.0580	0.2612	0.0024	0.0015	0.0020	0.0130	0.0013

Whether the $\delta^{11}B$ of corals is equal to that of $B(OH)_4^-$ has emerged as one of the main questions involved in these issues. A series of inorganic calcite precipitation experiments have shown that $B(OH)_4^-$ is the only or dominant species incorporated into calcite (Hemming et al., 1995; Sanyal et al., 1996, 2000). However, Klochko et al. (2009) recently found that both trigonal and tetrahedral coordinated boron existed in biogenic and hydrothermal carbonates. Rollion-Bard et al. (2011) also found both boron coordination species, but in different proportions depending on the coral microstructure, i.e. centres of calcification versus fibres. They suggested that careful sampling is necessary before performing boron isotopic measurements in deep-sea corals (Rollion-Bard et al., 2011). Inorganic calcite precipitation experiment has been carried out by Xiao et al. (2006a), indicating that the $\delta^{11}B$ of inorganic calcium carbonate was not parallel with the calculated curve of $B(OH)_4^-$, but deviated increasingly from the parallel trend as pH increased. When the pH was increased to a certain value, the isotopic fractionation factor of boron between precipitation and solution was greater than 1. Xiao et al. (2006a) reasoned that the presence of Mg^{2+} or other microelements was the main reason for this observation and concluded that $B(OH)_3$ incorporated preferentially into brucite. If this is true, the isotopic compositions of boron in corals can be affected by the existence of brucite in corals and the preferential incorporation of $B(OH)_3$ into brucite. If the brucite-bearing corals were used in the $\delta^{11}B$-pH proxy, the measured $\delta^{11}B$ of corals and the calculated pH will be higher than the normal value, which influences the $\delta^{11}B$-pH proxy negatively. However, little attention has been paid to the mechanism of boron incorporated into brucite and its influence on the boron isotopic composition of corals.

In this study, experiments on the incorporation of boron during the deposition of brucite from magnesium-free artificial seawater at various pH values were carried out. The incorporation species of boron into brucite and the the boron isotope fractionation during deposition of brucite were determined. The influence of brucite in corals on Mg/Ca and the $\delta^{11}B$, judgment method for existence of brucite in corals and its potential application in the $\delta^{11}B$-pH proxy and the Mg/Ca-SST proxy were discussed. This result will shed some light on the application of the Mg/Ca-SST proxy and the $\delta^{11}B$-pH proxy.

2 Methods

2.1 Reagents and equipment

1.0 M HCl, 0.5 M NaOH, and 0.5 M $MgCl_2$ were prepared using boron-free water with twice distilled HCl (GR), NaOH (GR), and $MgCl_2$ (GR), respectively. The concentration of the Cs_2CO_3 (99.994 % purity) solution used in our study was $12.3\,g\,Cs\,l^{-1}$. A suspended graphite solution was prepared using spectrum pure (SP) graphite mixed with 80 % ethanol and 20 % water. For a mannitol concentration of $1.82\,g\,l^{-1}$, GR mannitol mixed with boron-free water was used. The boron-free water was obtained by using 18.2 M Ω milliQ of water exchanged with an Amberlite IRA 743 boron specific resin. A GV IsoProbe T-single magnetic sector thermal ionization mass spectrometer was used for boron isotope analysis. A 2100 type and UV-2100 type spectrophotometer from Shanghai Unico Ltd was used for boron concentration analysis. A D/Max-2200 type X-ray diffraction equipment from Japan neo-confucianism company was used for XRD analysis. A TP310 type pH meter from Beijing Time Power Co. LTD was used for pH analysis.

Throughout all the experiments, vessels of Teflon, polyethylene or chert were used for avoiding boron contamination.

2.2 Magnesium-free artificial seawater

Magnesium-free artificial seawater was prepared by Mocledon prescription. The chemical composition of the magnesium-free artificial seawater is given in Table 1. In order to get sufficient quantities of boron for precise isotopic analysis in the precipitated $Mg(OH)_2$, boron concentration in the artificial seawater was adjusted to 45.9 ppm, approximately 10 times that of normal seawater (∼4.5 ppm). According to the result reported by Ingri et al. (1957), there was no polyborate species present when the boron concentration of aqueous solution was 45.9 ppm. The pH value and boron isotopic composition of the initial artificial seawater was 3.64 and -7.00 ± 0.07 ‰, respectively. Since magnesium-free artificial seawater was used in our experiments, no brucite was deposited while the pH was being adjusted. Brucite was deposited only when $MgCl_2$ was added after the pH adjustments were completed.

2.3 Experimental deposition of brucite

Deposition experiments were carried out in a pH-controlled system at a temperature of 22 ± 0.5 °C in a super-clean laboratory (100 Class). Firstly, about 200 ml of artificial seawater was placed inside a plastic beaker. Solutions of NaOH were slowly added to each beaker to achieve the following range of pH values: 9.5, 10.0, 10.5, 11.0, 11.5, 12.0, 12.5, and 13. 0. 8 ml of $MgCl_2$ solution was then added dropwise into the artificial seawater with different pH values. During this process, NaOH was added to keep the pH at the predetermined pH values as the brucite was deposited. The pH fluctuations were measured by a pH meter with a precision of 0.02. A magnetic stirrer was used during the experimental process to ensure the reactions were completed. The experiment was terminated after 8 ml of $MgCl_2$ was added. After mixing the deposit and solution well, the mixture was divided into two parts equally. One was filtrated by pumping immediately to isolate deposit from the solution (defined as a repose time $T_r = 0$ h) and the other was filtrated by pumping after reposing for 20 h (defined as a repose time $T_r = 20$ h). The separated solution was placed in air-tight plastic bottles, and the brucite deposit was washed with boron-free water until Cl^- was no longer detected. Then the deposited material was dried at 60 °C and placed in air-tight plastic bottles.

2.4 Separation of boron from the samples

In preparation for isotopic measurement, boron was extracted from the artificial seawater and the brucite using a two-step chromatographic technique (Wang et al., 2002). About 0.5 ml of Amberlite IRA 743 boron-specific resin with 80–100 mesh was placed in a polyethylene column with a diameter of 0.2 cm. The length of the resin bed was 1.5 cm. About 200 mg of brucite was first dissolved using a slightly excessive amount of boron-free HCl solution, passed through a column filled with Amberlite IRA 743 resin, and then eluted using approximately 5 ml of 0.1 M HCl at 75 °C. An amount of mannitol approximately equimolar to the boron content was added to the eluate, which was then desiccated to near dryness by partial evaporation in a super clean oven with laminar flow at 60 °C (Xiao et al., 2003). The solution was then loaded again into the column filled with a mixed resin composed of 0.5 ml cation-exchange resin (H^+ form) and 0.5 ml anion-exchange resin (ion- exchange II, HCO_3^- form). The boron was eluted by 5 ml of boron-free water. The eluate was evaporated again at 60 °C to produce a solution with a boron concentration of about 1 μg B μl^{-1} for isotopic measurement. The procedures for extracting boron in the liquid samples were the same as those described above. The total boron blank in chemical process and filament loading was determined by isotope dilution mass spectrometry (IDMS) to contain 46 ng of boron.

2.5 Measurements of boron concentration and isotopic composition

The boron concentrations were determined by the azomethine-H spectrophotometric method. One ml of sample solution, 2 ml of buffer solution, and 2 ml of azomethine-H solution were added in that order. After thorough mixing, each solution was allowed to stand for 120 min. The absorption of the boron-azomethine-H complex was measured at 420 nm using a spectrophotometer. The external precision of the azomethine-H method used here was 2 %.

The isotopic compositions of boron in all samples were measured by a GV IsoProbe T single magnetic sector thermal ionization mass spectrometer and the P-TIMS method using $Cs_2BO_2^+$ ions with a graphite loading (Xiao et al., 1988). Two μl of graphite slurry was first loaded onto a degassed tantalum filament, and then approximately 1 μl of sample solution containing about 1–4 μg of boron and an equimolar amount of mannitol were also loaded. This was followed by 1–2 μl of a Cs_2CO_3 solution containing an equimolar amount of cesium. The loaded material was dried by heating the filament at 1.2 A for 5 min.

The data were collected by switching the magnetic field between the masses 308 ($^{133}Cs_2^{10}B^{16}O_2^+$) and 309 ($^{133}Cs_2^{11}B^{16}O_2^+$), and the intensity ratios of the ion beams at masses 308 and 309 ($R_{309/308}$) were calculated. Calibrated with oxygen isotopes, the $^{11}B/^{10}B$ ratio was calculated as $R_{309/308} - 0.00078$. The isotopic composition of boron was expressed as an $\delta^{11}B$ value according to the following formula:

$$\delta^{11}\mathrm{B}\ (‰) = \left[\left(^{11}\mathrm{B}\Big/^{10}\mathrm{B}\right)_{\mathrm{sample}}\Big/\left(^{11}\mathrm{B}\Big/^{10}\mathrm{B}\right)_{\mathrm{standard}} - 1\right] \times 1000$$

Here the standard material is NIST SRM 951, the recommended value of which is 4.04362 ± 0.00137 (Catanzaro et al., 1970). The measured average $\delta^{11}B/^{10}B$ ratio of NIST SRM 951 was 4.0525 ± 0.0027 ($2\sigma_m$, $n = 5$).

3 Results and discussion

3.1 Dissolved boron species and boron isotope in seawater

The dominant aqueous species of boron in seawater are $B(OH)_3$ and $B(OH)_4^-$. The relative proportions of these species are a function of pH (Fig. 1a) and given by the following relation:

$$B(OH)_3 + H_2O \leftrightarrow B(OH)_4^- + H^+ \quad (1)$$

Figure 1 shows the theoretical distribution of boron species as a function of pH for seawater. At low pH (pH < 7), virtually all of the boron in seawater is in the $B(OH)_3$ species; conversely, at high pH (pH > 10), virtually all of the boron

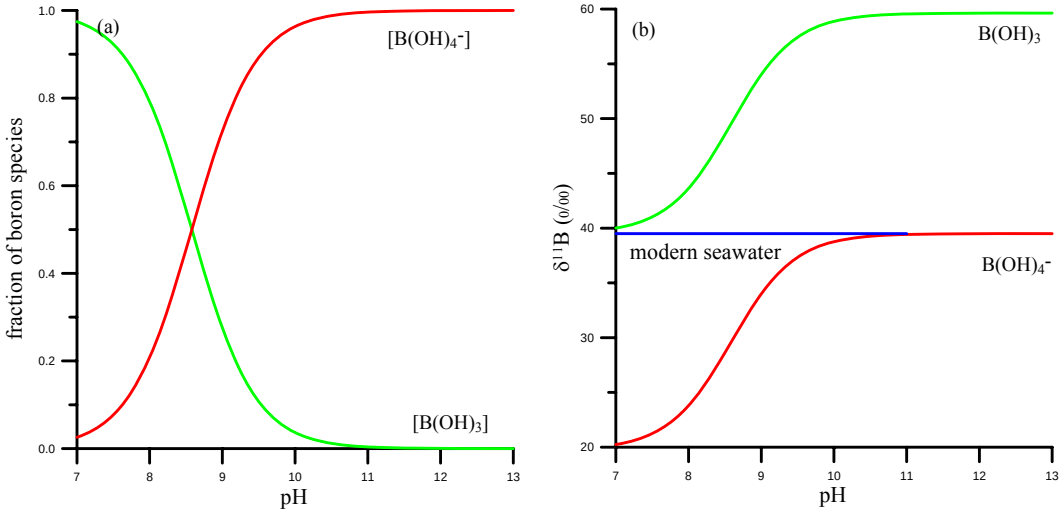

Fig. 1. Fraction **(a)** of the major dissolved boron species $B(OH)_3$ (green curve) and $B(OH)_4^-$ (red curve) in seawater, using $pK_b = 8.597$ (Dickson, 1990) and stable boron isotope fractionation **(b)** between them as a function of pH, using $\alpha_{4-3} = 0.974$ (Klochko et al., 2006). At low pH (pH < 7), virtually all of the boron in seawater is in the $B(OH)_3$ species; conversely, at high pH (pH > 10), virtually all of the boron is in the $B(OH)_4^-$ species (Fig. 1a). Only the $B(OH)_4^-$ incorporated into the marine bio-carbonates is one of the essential hypotheses for using boron isotopic composition in marine bio-carbonate to reconstruct the paleo-environment (Hemming and Hanson, 1992).

is in the $B(OH)_4^-$ species (Fig. 1a). The isotope exchange reaction between these species is given by:

$$^{10}B(OH)_3 + {}^{11}B(OH)_4^- \leftrightarrow {}^{11}B(OH)_3 + {}^{10}B(OH)_4^- \quad (2)$$

The distribution of species and the isotope exchange reaction are solved simultaneously to give the isotopic composition of the individual boron species vs. pH for seawater (Fig. 1b). The abundances of two stable isotopes ^{11}B and ^{10}B at pH 8 make up approximately 80 % and 20 % of the total boron, respectively. Modern seawater has a boron concentration of about 4.5 ppm, and a consistent, worldwide $\delta^{11}B$ isotopic composition of $+39.61 \pm 0.04$‰ relative to NIST SRM 951 (Foster et al., 2010). The isotopic composition of $B(OH)_4^-$ increases with pH and so does the $\delta^{11}B$ of carbonates, provided that $B(OH)_4^-$ is preferentially incorporated in the carbonates. As a result, variations of seawater pH in the past should be traceable by variations of $\delta^{11}B$ in fossil carbonates. This is the basis of the boron paleo-pH proxy (Hemming and Hanson, 1992).

3.2 The partition coefficient of boron between Brucite and final seawater

The boron concentrations and the partition coefficients (K_d) between brucite and final seawater are listed in Table 2, and shown in Fig. 2. The results are shown as follows:

1. The variation trend of the results for $T_r = 0$ h and $T_r = 20$ h are basically the same (Fig. 2a), indicating the incorporation of boron into brucite deposit is instantaneous, and the reaction time is not a main limiting factor. This finding is consistent with the previous study (Liu et al., 2004).

2. When the pH is lower than 10, $[B]_{fsw}$ decreases as the pH increases, and reaches the lowest value at pH 10 (Fig. 2a). This indicates that the amount of boron incorporated into deposited brucite increases as the pH increases, and reaches the highest value at pH 10. $[B]_{fsw}$ increases quickly at higher pH values, and no smooth trend is observed, indicating that the amount of incorporated boron decreases quickly.

3. When pH is lower than 10, K_d increases as the pH increases (Fig. 2b). The K_d reaches its highest values of 487.5 and 494.2 for $T_r = 0$ h and $T_r = 20$ h at pH 10, respectively. When the pH is higher than 10, K_d decreases and shows a mild trend after pH 12.

The K_d between brucite deposit and final seawater can be shown as:

$$K_d = (f \times K_{d3} + K_{d4}) / (1 + f) \quad (3)$$

$K_d = \{[B_3]_{solid} + [B_4]_{solid}\}/\{[B_3]_{fluid} + [B_4]_{fluid}\}$,
$K_{d3} = [B_3]_{solid}/[B_3]_{fluid}$, $K_{d4} = [B_4]_{solid}/[B_4]_{fluid}$,
$f = [B_3]_{fluid}/[B_4]_{fluid}$, K_{d3} and K_{d4} are the partition coefficient of $B(OH)_3$ and $B(OH)_4^-$, respectively. f_3 is the ratio of $B(OH)_3$ to $B(OH)_4^-$ in solution. This equation indicates that K_d is not only related with K_{d3} and K_{d4}, but also with the fraction of $B(OH)_3$ in solution. The K_d between clay minerals and seawater is 3.60 at $T = 5$ °C and pH 8.45 (Palmer et al., 1987), but the highest K_d in our experiments is 494 at pH 10, which is much higher than 3.6. It indicates

Table 2. Boron concentration (ppm) and partition coefficient K_d between brucite deposit and final seawater.

T_{repose}	pH	9.5	10.0	10.5	11.0	11.5	12.0	12.5	13.0
0 h	$[B]_{fsw}$	4.60	1.92	2.59	4.63	10.3	15.6	21.7	22.9
	$[B]_d$	901	938	845	626	658	290	274	250
	K_d	196	488	326	135	64.2	18.6	12.6	10.9
20 h	$[B]_{fsw}$	5.16	1.93	3.17	5.80	15.3	20.8	21.7	24.6
	$[B]_d$	1859	952	885	844	685	413	326	229
	K_d	360	494	279	146	44.8	19.9	15.0	9.31

$[B]_{fsw}$ and $[B]_d$ are the boron concentrations in final seawater and deposit, respectively.

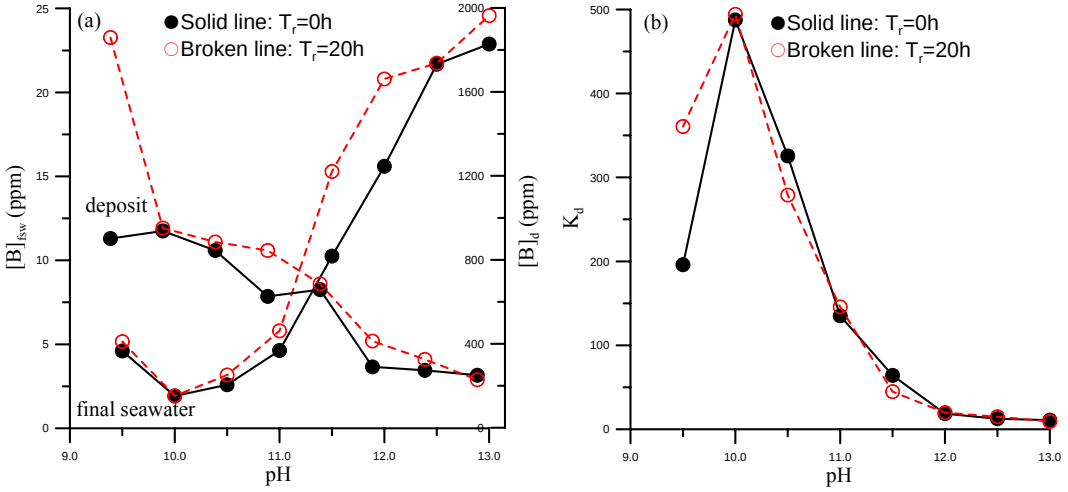

Fig. 2. Boron concentrations **(a)** and partition coefficient K_d **(b)** between brucite deposit and final seawater for $T_r = 0$ h and 20 h. The variation trend of the results for $T_r = 0$ h and $T_r = 20$ h are basically the same (Fig. 2a), indicating that the incorporation of boron into brucite deposit is instantaneous. $[B]_{fsw}$ decreases firstly and then increases quickly with the lowest value at pH 10 (Fig. 2a), indicating the amount of boron incorporated into deposited brucite increases firstly and decrease as pH increases, and reaches the highest value at pH 10. The variation trend of K_d is contrary to that of $[B]_{fsw}$ (Fig. 2b).

that the K_{d3} is much greater than K_{d4}, i.e. the incorporation capacity of $B(OH)_3$ into brucite is much higher than that of $B(OH)_4^-$ and the K_{d3} contribution is dominating. The quantity of brucite reaches its highest at pH 10, indicating the reaction equivalence point of brucite deposition occurs approximately at pH 10. The K_d also reaches its highest at pH 10. When pH is higher than 10, the f and K_{d3} decreases while K_{d4} increases as the increasing pH. Although the increasing concentration of OH^- in solution can influence the adsorption of $B(OH)_4^-$ (Keren et al., 1981), the adsorption of $B(OH)_4^-$ continues, and the K_{d4} still increases perhaps. Because of K_{d3} is greater than K_{d4}, the decreasing of K_{d3} is dominating, so that the K_d decreases with the increasing pH. In the study of Xu and Ye (1997), the point of zero charge (PZC) of brucite is close to 11.9, which approximates to the inflexion point (pH 12) in our experiment. When the pH is higher than PZC, anions will not be adsorbed by goethite and gibbsite (Kingston et al., 1972), so that the adsorption ability of $B(OH)_4^-$ by brucite decreases greatly when the pH is higher than the PZC of brucite. Therefore, K_d should monotonically decrease with increasing pH as well.

Boron removal experiments by magnesium hydroxide at different pH values have been carried out by Liu et al. (2004), de la Fuente and Muñoz (2006) and Yuan et al. (2006). They attributed the adsorption of $B(OH)_4^-$ to the magnesium hydroxide. Their results showed that $[B]_{fsw}$ reached its lowest values at pH 9.3 or 10, which indicates that adsorption had reached its highest values. The $[B]_{fsw}$ then increased slowly at higher pH values. The results of the present study are consistent with their work.

There is a slight difference in the variation of $[B]_d$ with pH for different T_r values. When $T_r = 0$ h and pH = 9.5, $[B]_d$ is slightly lower than that at pH 10, and the highest $[B]_d$ value of 937.8 ppm also appears at pH 10. But when $T_r = 20$ h, the maximum $[B]_d$ may appear at pH $\leq$ 9.5, while the highest value at pH 9.5 is 1859 ppm, which is much higher than 951.5 ppm at pH 10. Considering the slight difference in the

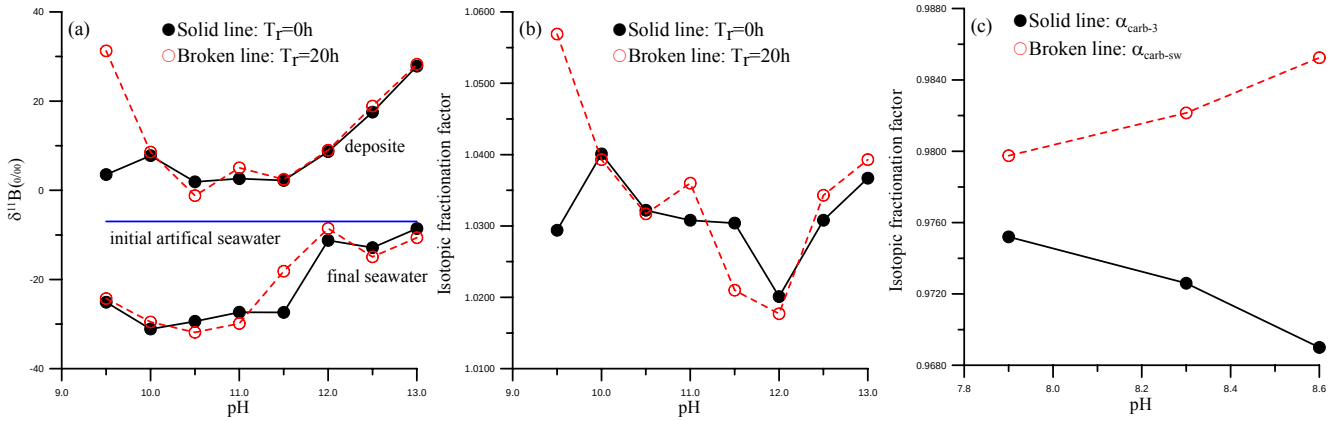

Fig. 3. Isotopic compositions **(a)** and fractionation factor (α_{d-fsw}) **(b)** of boron between brucite deposit and solution for $T_r = 0$ h and 20 h and **(c)** between inorganic carbonate and seawater (Sanyal et al., 1996). The variation trend of $\delta^{11}B$ for $T_r = 0$ h and $T_r = 20$ h are basically same and all the $\delta^{11}B_d$ values are enriched in the heavy isotope relative to the $\delta^{11}B_{fsw}$ **(a)**. All the α_{d-fsw} are greater than 1 and shows a waved pattern **(b)**, which is entirely different from that of the carbonates deposits **(c)**.

boron balance time of the deposited $Mg(OH)_2$, the value for $T_r = 20$ h may be more reliable.

The evolution pattern of boron incorporated into the $Mg(OH)_2$, and the variations in partition coefficients with the pH, are basically the same as those of oxides and clay minerals. However, the maximum amounts of incorporated boron in brucite or other hydroxides are much higher than those of the oxides and clay minerals (Keren et al., 1981; Keren and Gast, 1983; Goldberg and Glaubig, 1985, 1986; Lemarchand et al., 2005, 2007), indicating that the incorporation capacity of boron on hydroxides is stronger than that of both oxides and clay minerals. The boron concentration in corals varies from 39 to 117.5 ppm (Vengosh et al., 1991; Gaillardet and Allègre, 1995; Xiao et al., 2006b; Liu et al., 2009). If 4.5 ppm of the seawater boron concentration is used, the K_d between coral and seawater varies from 8.7 to 26.1. In our experiments, the boron concentration in the initial artificial seawater is 45.9 ppm, finally the level of boron concentration in brucite depositions can be divided by 10. In this case, the expected boron content would range between 22 and 95 ppm (excluding the aberrant value of 185.9 ppm obtained at pH 9.5), so the K_d between brucite and final seawater varies from 4.8 to 19.2. Such a range of boron concentrations and K_d is of the same order of magnitude as the common boron contents measured in corals.

3.3 Isotopic fractionation of boron between deposited brucite and solution

Isotopic compositions of boron in deposited brucite ($\delta^{11}B_d$) and final seawater ($\delta^{11}B_{fsw}$) are listed in Table 3 and shown in Fig. 3. The crucial points illustrated in Fig. 3 are summarized as follows:

1. The variation trend of the results for $T_r = 0$ h and $T_r = 20$ h are basically same (Fig. 3a). This indicates that the isotopic balance between brucite deposit and solution is instantaneous, and that the results of the experiment are exact. A minor difference between $T_r = 0$ h and $T_r = 20$ h appears as the pH increases from 9.5 to 10.0. When $T_r = 0$ h, $\delta^{11}B_d$ and α_{d-fsw} both increase as the pH increases from 9.5 to 10.0. However, when $T_r = 20$ h, $\delta^{11}B_d$ and α_{d-fsw} both decrease as the pH increases from 9.5 to 10.0. This is perhaps related to the fact that the formation of brucite is slower at low pH than at high pH.

2. All the $\delta^{11}B_d$ values are enriched in the heavy isotope relative to the $\delta^{11}B_{fsw}$ (Fig. 3a). All the α_{d-fsw} are greater than 1 (Fig. 3b), which is entirely different from those of the carbonates deposits (Fig. 3c). As $B(OH)_4^-$ is incorporated preferentially into carbonate deposits, all the $\delta^{11}B$ values of carbonates are lower than that of the parent seawater. Meanwhile, all the isotopic fractionation factors $\alpha_{carb-sw}$ between carbonates and seawater are lower than 1 and increase with pH. In this study, the α_{d-fsw} between brucite deposit and solution shows a waved pattern (Fig. 3b), suggesting a complex isotopic fractionation process.

   The $\delta^{11}B_d$, $\delta^{11}B_{isw3}$ and $\delta^{11}B_{isw4}$ of $B(OH)_3$ and $B(OH)_4^-$ in initial seawater, calculated using the different α_{4-3} versus pH values of the parent solutions, are shown in Fig. 4. When $T_r = 0$ h, the $\delta^{11}B_d$ values are equal to or lower than the $\delta^{11}B_{isw3}$ calculated using $\alpha_{4-3} = 0.9600$. When $T_r = 20$ h, the $\delta^{11}B_d$ values are equal to or lower than the $\delta^{11}B_{isw3}$ calculated using $\alpha_{4-3} = 0.9397$, but all the $\delta^{11}B_d$ values are higher than $\delta^{11}B_{isw}$ (Fig. 4). The α_{4-3} of 0.9600 and 0.9397 is calculated according to the highest $\delta^{11}B$ of deposited brucite for $T_r = 0$ h and $T_r = 20$ h. If $\delta^{11}B_d$ is equal to $\delta^{11}B_{isw3}$, it implies that only $B(OH)_3$ is

Table 3. Isotopic fractionation of boron between deposited brucite and solution.

Repose time	0 h			20 h		
pH	$\delta^{11}B_d$ (‰)	$\delta^{11}B_{fsw}$ (‰)	α^{b}_{d-fsw}	$\delta^{11}B_d$ (‰)	$\delta^{11}B_{fsw}$ (‰)	α^{b}_{d-fsw}
9.5	$3.54 \pm 0.1(2)^a$	$-25.09 \pm 0.1(2)$	1.0294	31.27(1)	−24.27(1)	1.0569
10.0	$7.77 \pm 0.5(2)$	$-31.11 \pm 0.1(2)$	1.0401	8.57(1)	−29.53(1)	1.0393
10.5	$1.89 \pm 0.1(2)$	$-29.38 \pm 0.2(2)$	1.0322	$-1.20 \pm 0.3(2)$	−31.85(1)	1.0317
11.0	$2.61 \pm 0.1(2)$	$-27.33 \pm 0.5(2)$	1.0308	5.04(1)	−29.87(1)	1.0360
11.5	$2.21 \pm 0.3(3)$	$-27.38 \pm 0.5(3)$	1.0304	2.45(1)	$-18.15 \pm 0.5(2)$	1.0210
12.0	$8.67 \pm 0.1(2)$	$-11.23 \pm 0.3(2)$	1.0201	8.99(1)	−8.55(1)	1.0177
12.5	$17.53 \pm 0.1(2)$	$-12.86 \pm 0.6(2)$	1.0308	18.89(1)	−14.92(1)	1.0343
13.0	$27.84 \pm 0.2(3)$	$-8.58 \pm 0.7(2)$	1.0367	$28.26 \pm 0.4(2)$	−10.63(1)	1.0393

[a]The number in brackets indicate measurement times;

[b]α_{d-fsw} is the isotopic fractionation factor of boron between deposit and final seawater, calculated as $\alpha_{d-fsw} = (1000 + \delta^{11}B_d)/(1000 + \delta^{11}B_{fsw})$.

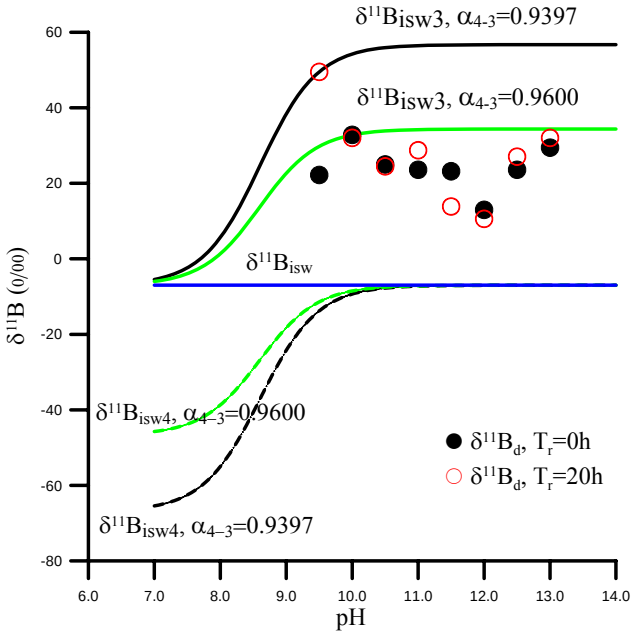

Fig. 4. $\delta^{11}B$ of brucite deposit ($\delta^{11}B_d$), and $\delta^{11}B$ of $B(OH)_3$ ($\delta^{11}B_{isw3}$) and $B(OH)_4^-$ ($\delta^{11}B_{isw4}$) in initial seawater calculated using different α_{4-3} versus pH values of the parent solution. When $T_r = 0$ h, the $\delta^{11}B_d$ values (black solid circle) are equal to or lower than the $\delta^{11}B_{isw3}$ calculated using $\alpha_{4-3} = 0.9600$ (black line). When $T_r = 20$ h, the $\delta^{11}B_d$ values (red circle)are equal to or lower than the $\delta^{11}B_{isw3}$ calculated using $\alpha_{4-3} = 0.9397$ (green line), but all the $\delta^{11}B_d$ values are higher than $\delta^{11}B_{isw}$ (blue line).

incorporated into $Mg(OH)_2$, which is impossible under normal circumstances. Moreover a situation in which $\delta^{11}B_d > \delta^{11}B_{isw3}$ would be even more improbable. Except for pH 9.5, $\delta^{11}B_d$ values are lower than $\delta^{11}B_{isw3}$ calculated using $\alpha_{4-3} = 0.9600$ (Fig. 4), so that the true α_{4-3} would have to be lower than 0.9600, which is a little lower than the currently expected value between 0.983 (Sanchez-Valle et al., 2005) and 0.952 (Zeebe, 2005). The pH values used in previous carbonate precipitation experiments are lower than 9.0, while that of our experiments are between 9.5 and 13.0. The differences of the experiments conditions may result diverse α_{4-3}, but which value is much more reliable or the true α_{4-3} is still uncertain. Our results also indicate that $\delta^{11}B_d$ is not parallel with $\delta^{11}B_{isw3}$, but first decreases and then increases with an inflexion at pH 12. All of the data indicate that both $B(OH)_3$ and $B(OH)_4^-$ are incorporated into the deposited brucite.

The fractions of $B(OH)_3$ (F_{d3}) in the brucite deposit calculated using $\alpha_{4-3} = 0.9397$ and $\alpha_{4-3} = 0.9600$ are shown in Fig. 5. It seems that F_{d3} tends to decrease with decreasing α_{4-3}. Because the adopted α_{4-3} is not true, the calculated F_{d3} is not exact. The true F_{d3} could be lower than the value indicated in Fig. 5, but the variation trend of F_{d3} with pH should be certain and much higher than that of the initial artificial seawater (F_{isw3}). The $\delta^{11}B_d$ is the concurrent result of $\delta^{11}B_{d3}$ and $\delta^{11}B_{d4}$. Here $\delta^{11}B_d$ can be shown as:

$$\delta^{11}B_d = f_{d3} \times \delta^{11}B_{d3} + (1 - f_{d3}) \times \delta^{11}B_{d4} \quad (4)$$

where f_{d3} is the fraction of $B(OH)_3$ in solid. During pH 10–12, both $\delta^{11}B_{d3}$ and $\delta^{11}B_{d4}$ increases with increasing pH (Fig. 1b). Therefore, the $\delta^{11}B_d$ should be increased with the increasing pH, but the increasing trend is inconspicuous (Fig. 3a). There are two reasons accounting for this. On the one hand, the increasing $\delta^{11}B_{d3}$ and $\delta^{11}B_{d4}$ can result in the increasing of $\delta^{11}B_d$. On the other hand, with the increasing pH, the dominant decreasing incorporation fraction of $B(OH)_3$ and increasing incorporation fraction of $B(OH)_4^-$ will result the deceasing of $\delta^{11}B_d$. With the common influence of these two aspects, the variation of $\delta^{11}B_d$ with pH is small. When the pH reaches 12 (PZC of brucite),

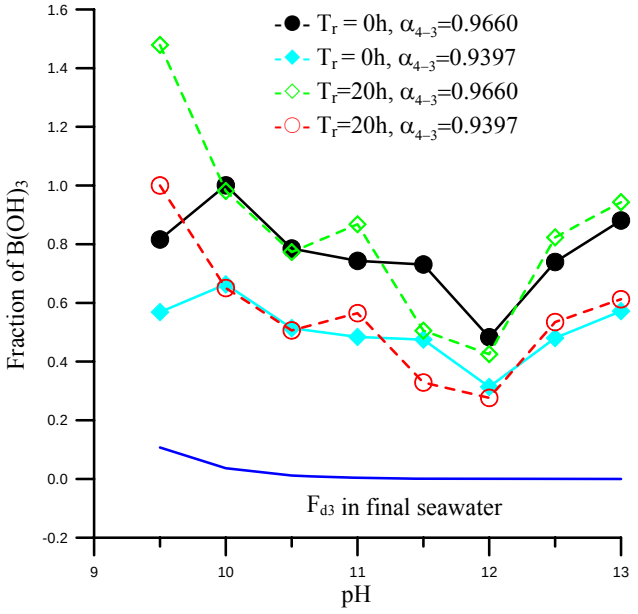

Fig. 5. Fraction F_{d3} of $B(OH)_3$ in brucite deposit and final seawater calculated according to $\delta^{11}B_d$ with different α_{4-3}. The variation trend of F_{d3} for a different repose time is basically the same. F_{d3} tends to decrease with decreasing α_{4-3} and is much higher than that of the initial artificial seawater (blue curve).

the adsorption quantity of $B(OH)_4^-$ decreases suddenly, while that of $B(OH)_3$ increases (Fig. 5). So the $\delta^{11}B_d$ increases.

3. The manner in which α_{d-fsw} changes with pH for $T_r = 0$ h and 20 h is shown in Fig. 3b. Except for pH 9.5, both patterns are basically the same for each T_r, and match the change in F_{d3} shown in Fig. 5. The α_{d-fsw} values decrease as the pH increases from 9.5 to 12, and reaches the lowest point at pH 12. Then α_{d-fsw} values increase rapidly. The α_{d-fsw} reflects the relative ratio of $B(OH)_3$ to $B(OH)_4^-$ in brucite.

   The explanation of $\delta^{11}B_d$ with pH can be also used for the explanation of the boron fractionation factor between brucite and solution. When the pH ranges from 10 to 12, the incorporation fraction of $B(OH)_3$ decreases continuously (Fig. 5), which is contrary to that of $B(OH)_4^-$. This lead to the deceases ratio of $B(OH)_3$ to $B(OH)_4^-$, so the α_{d-sw} decreases. When pH reaches 12 (PZC of $Mg(OH)_2$), the adsorption quantity of $B(OH)_4^-$ decreases suddenly, and the relative ratio of $B(OH)_3$ to $B(OH)_4^-$ increases (Fig. 5), so the α_{d-fsw} also increases.

   Our results indicate that $B(OH)_3$ is preferentially incorporated into the solid phase during the deposition of brucite. In a precipitated experiment of calcium carbonates from artificial seawater, Xiao et al. (2006a) obtained the result that the boron isotopic fractionation factors between calcium carbonates and seawaters were higher than 1. They reasoned that the presence of Mg^{2+} or other microelements was the main reason for this observation and concluded that the heavier $B(OH)_3$ species was incorporated preferentially into $Mg(OH)_2$. The results of our study have further confirmed the conclusion of Xiao et al. (2006a).

4 Model of boron incorporated into brucite

4.1 Model 1: boron adsorption by minerals

The boron adsorption by minerals can be explained by phenomenological equation (Keren et al., 1981). It is supposed that when $B(OH)_3$, $B(OH)_4^-$ and OH^- coexist in solution, they can be adsorbed by $Mg(OH)_2$, metal oxides and clay minerals, and the affinity coefficients K_{B3}, K_{B4} and K_{OH} are $K_{B3} < K_{B4} < K_{OH}$ for $B(OH)_3$, $B(OH)_4^-$ and OH^-, respectively (Keren et al., 1981). They compete for the same adsorption site on solid. When the pH is less than 7, $B(OH)_3$is dominant. Because K_{B3} to clay mineral is very low, the boron adsorption is relatively minor. Under this pH value, the concentration of $B(OH)_4^-$ and OH^- is very low. Although they have a relatively stronger affinity to clay, their contribution to the total boron adsorption is still very small. When the pH increases to 9, $B(OH)_4^-$ concentration increases rapidly. Compared with $B(OH)_4^-$, OH^- concentration is still lower. So the adsorbed boron increases rapidly. When the pH further increases, OH^- concentration will increase evidently, and the boron contribution decreases because of the competition for adsorption site with $B(OH)_4^-$.

In this study, when the pH is lower than 10, K_d increases as the pH increases (Fig. 2b). The K_d reaches its highest values at pH 10. When the pH is higher than 10, K_d decreases and shows a mild trend after pH 12. The variation characteristics of K_d with the pH can also be explained partly by this model. But isotopic fractionation characteristics of boron, the maximum adsorption value and K_d value of brucite deposit can not be explained by this totally.

The incorporation of $B(OH)_4^-$ into brucite may be related to adsorption. Previous studies (Liu et al., 2004; Garcia-Soto and Camacho, 2006; Yuan et al., 2006) have indicated that the incorporation of boron into brucite or MgO was an adsorption process. When Mg^{2+} exists in solution, it can be adsorbed by brucite crystallite, and the resulting positive charge can adsorb the negatively charged $B(OH)_4^-$. The equation is shown as follows:

$$\{[Mg(OH)_2]_m \cdot n\, Mg^{2+}\}^{2n+} + xB(OH)_4^- \rightarrow \{[Mg(OH)_2] \cdot n\, Mg^{2+} \cdot xB(OH)_4^-\}^{2n-x} \downarrow \quad (5)$$

If model 1 is applied, the $\delta^{11}B_d$ should be lower than $\delta^{11}B_{isw}$ and α_{d-sw} should be lower than 1. In this study, however, the results show that all $\delta^{11}B_d$ are higher than

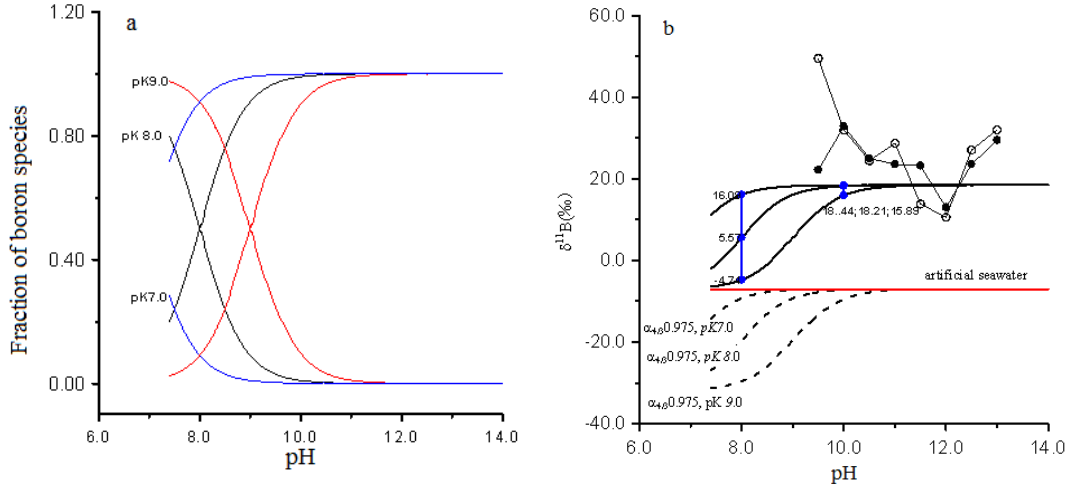

Fig. 6. The fraction **(a)** and δ^{11}B **(b)** of boron species calculated using different pK_a versus pH values. The influence of pK_a on fraction and δ^{11}B of boron species is big for a solution with the pH < 10. When the pH > 10, the influence of pK_a is insignificant. For example, the $\delta^{11}B_{isw3}$ calculated using pK_a 7.0, 8.0 and 9.0 ($\alpha_{4/3} = 0.975$) are 16.08 ‰, 5.57 ‰ and −4.74 ‰, respectively for pH 8 and 18.44 ‰, 18.21 ‰ and 15.89 ‰, respectively, for pH 10. When the pH > 11, there are basically no differences among them (Fig. 6b).

$\delta^{11}B_{isw}$ and α_{d-sw} values are higher than 1. This suggests that model 1 is not suitable to explain all the data in our study.

The apparent pH dependence of the fractionation between carbonates and clays can be described in terms of the α_{3-4} and the pK_a of the boric acid-borate equilibrium (Sanchez-Valle et al., 2005). This model explains the B isotopic fractionation data for inorganically and biologically precipitated carbonates and clays, and suggests that in minerals like clay and other layered hydroxides, surface charge properties play an important role by changing the apparent acid-base equilibrium constant.

In our study, pK_a of the boric acid-borate equilibrium may be affected due to the presence of a positive charge on the $Mg(OH)_2$ surface. The fraction and δ^{11}B of boron species calculated using different pK_a versus pH values is shown in Fig. 6, which suggests that the influence of pK_a on fraction and δ^{11}B of boron species is big for a solution with the pH < 10. When the pH > 10, the influence of pK_a is insignificant. For example, the $\delta^{11}B_{isw3}$ calculated using pK_a 7.0, 8.0 and 9.0 ($\alpha_{4/3} = 0.975$) are 16.08 ‰, 5.57 ‰ and −4.74 ‰, respectively for pH 8, and 18.44 ‰, 18.21 ‰ and 15.89 ‰, respectively for pH 10. When the pH > 11, there are basically no differences among them. The pH values of our experiments are higher 10, so the isotopic fractionation characteristics of boron are not attributed to the change of pK_a.

4.2 Model 2: chemical reaction of $B(OH)_3$ with $Mg(OH)_2$

Rodionov et al. (1991) reported that when limewater was added to seawater, $CaO \cdot B_2O_3 \cdot nH_2O$ was deposited. This reaction is shown as follows:

$$2\,H_3BO_3 + Ca(OH)_2 + aq \rightarrow CaO \cdot B_2O_3 \cdot nH_2O + aq \quad (6)$$

During deposition of brucite, a similar reaction may occur. $MgO \cdot B_2O_3 \cdot nH_2O$ may also be deposited. This hypothesis was confirmed by the XRD analyses of brucite. Compared with Fig. 7b, the brucite peak in Fig. 8 is clear, with apparent peaks of pinnoite ($Mg(BO_2)_2 \cdot 3H_2O$) and szaibelyite ($MgBO_2(OH)$). Judging from the quantity and intensity of these peaks, pinnoite content should be higher than that of szaibelyite. As the pH increases, the borate peak gradually weakens (Fig. 7c–h). When the pH is 12.5 (Fig. 7h), its peak is very close to that of $Mg(OH)_2$, though the characteristic pinnoite peak is still observed. The pinnoite is the result of the following reaction between brucite and H_3BO_3:

$$2\,H_3\,BO_3 + Mg(OH)_2 \rightarrow Mg(BO_2)_2 \cdot 3\,H_2O + H_2O \quad (7)$$

The above reaction cannot occur for $B(OH)_4^-$. Thus, F_{d3} can exceed F_{fsw3} due to the preferential incorporation of H_3BO_3 into $Mg(OH)_2$, which enriches the deposited brucite in ^{11}B. The presence of szaibelyite may be the result of $B(OH)_4^-$ adsorption.

If model 2 is applied, the $\delta^{11}B_d$ should be higher than $\delta^{11}B_{isw}$and α_{d-sw} values should be higher than 1. Furthermore, $\delta^{11}B_d$ and α_{d-sw} should decrease with increasing pH values. In our study, all the $\delta^{11}B_d$ values are enriched in the heavy isotope compared relative to the $\delta^{11}B_{fsw}$ (Fig. 3a), and

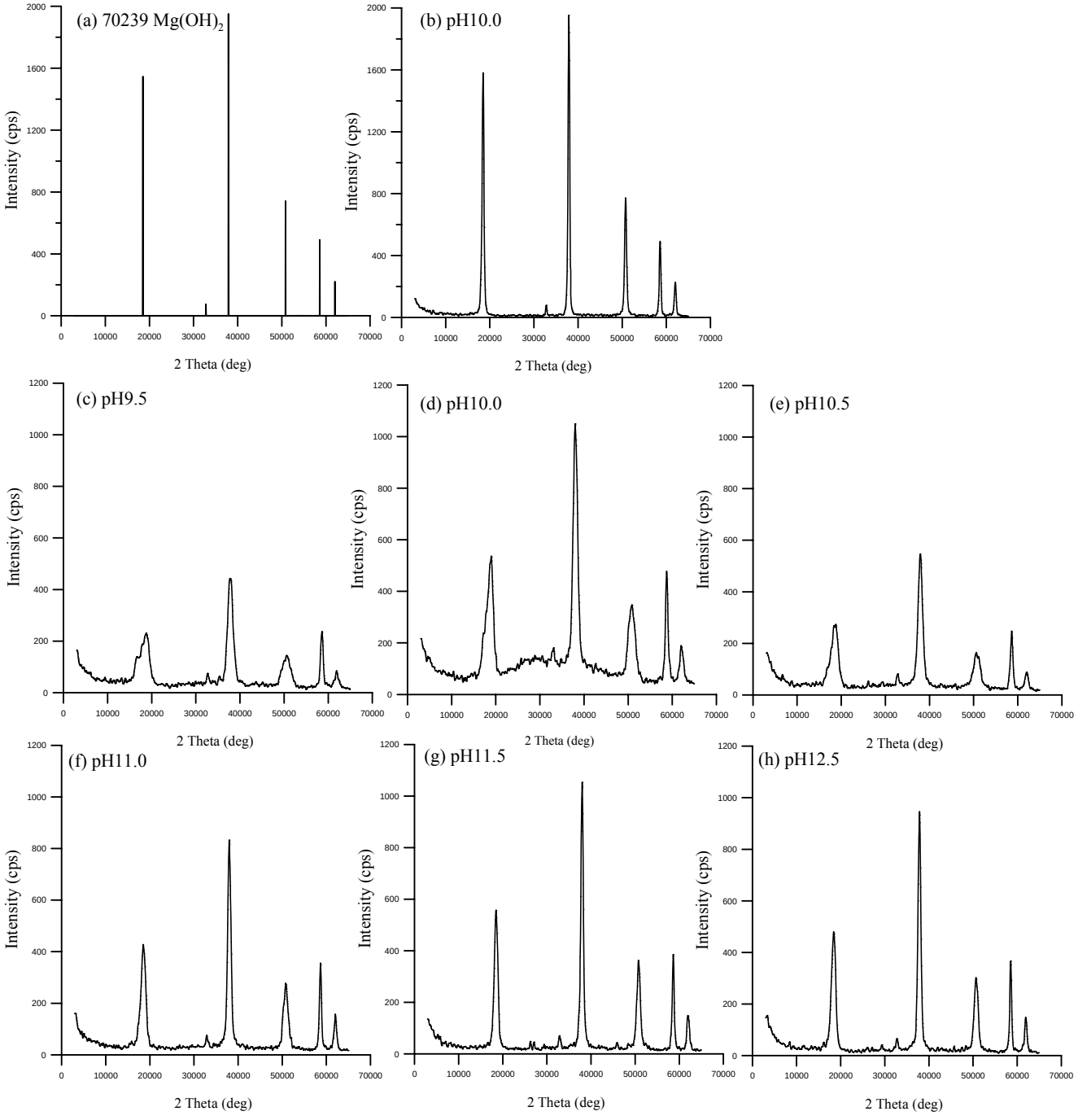

Fig. 7. X-Ray diffractogram of brucite deposited from artificial seawater at different pH values. **(a)** XRD of brucite standard, **(b)** XRD of brucite from boron-free artificial seawater at pH 10.0, **(c)–(h)** XRD of brucite in our experiments. The brucite peak in our samples is clear compared with the brucite standard **(a)**.

all the α_{d-fsw} are greater than 1 (Fig. 3b), which are consistent with model 2. But the α_{d-fsw} shows a waved pattern (Fig. 3b), which indicates a complex isotopic fractionation process and cannot be explained completely by model 2.

The fraction of boric acid in solution is negligible at high pH values (Fig. 1a), so that the amount of $B(OH)_3$ incorporated into brucite should be little. But the F_{d3} is much higher than the F_{isw3} (Fig. 5). This may be related to the transformation of borate to boric acid. After $B(OH)_3$ is incorporated into brucite, F_{isw3} decreases. In order to keep the balance of the $B(OH)_3/B(OH)_4^-$ ratio, $B(OH)_4^-$ in solution would transform to $B(OH)_3$. Meanwhile, the total boron

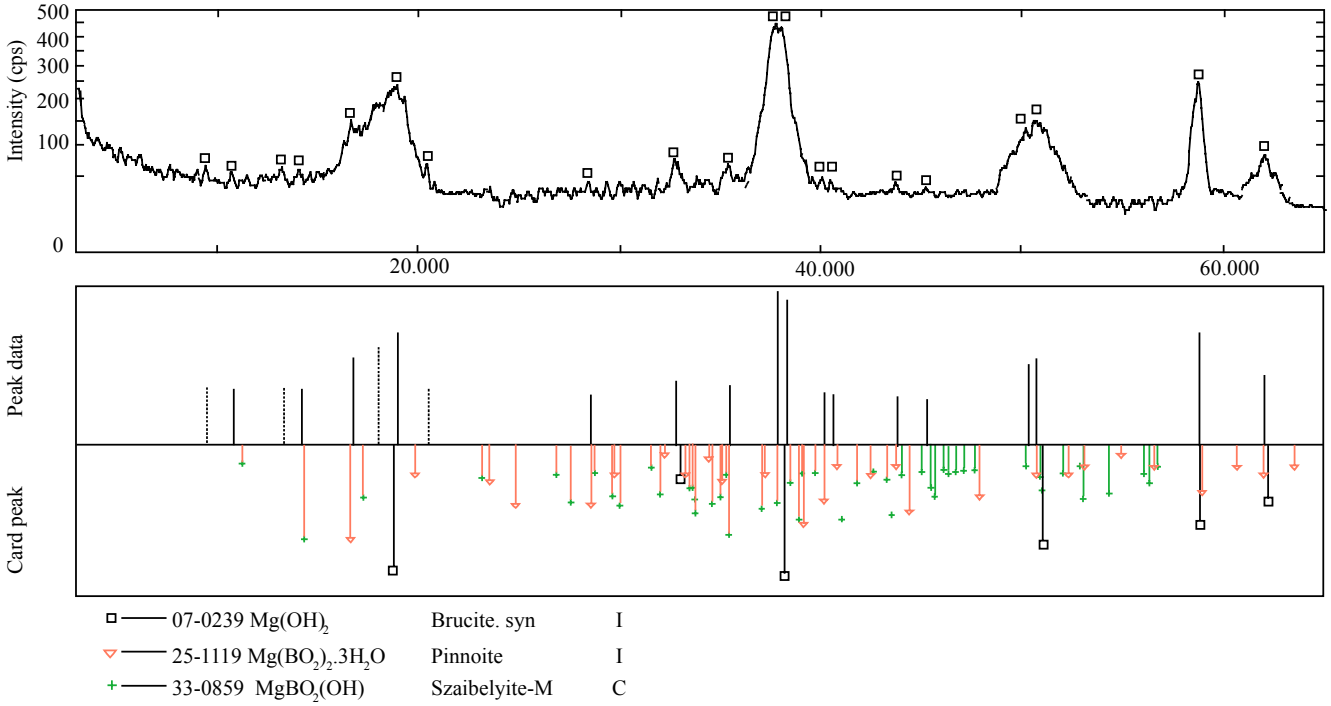

Fig. 8. X-Ray diffractogram of brucite deposited from B-containing artificial seawater at pH 9.5. It is a magnified figure of Fig. 7c. Compared with Fig. 7b, the brucite peak in Fig. 8 is clear, with apparent peaks of pinnoite ($Mg(BO_2)_2 \cdot 3H_2O$) and szaibelyite ($MgBO_2(OH)$). Judging from the quantity and intensity of these peaks, pinnoite content should be higher than that of szaibelyite. As the pH increases, the borate peak gradually weakens (Fig. 7c–h). When the pH is 12.5 (Fig. 7h), its peak is very close to that of $Mg(OH)_2$ standard (Fig. 7a), although the characteristic pinnoite peak is still observed.

quantity in solution decreases compared with initial solution. When a new equilibrium is reached, $B(OH)_3$ continues to incorporate into brucite, and $B(OH)_4^-$ in solution will transform to $B(OH)_3$ to keep the equilibrium. This process will repeat, and finally the F_{d3} is much higher than the F_{isw3}. However, the total boron quantity in solution is much less than that in the initial solution.

4.3 Model 3: both chemical reaction and adsorption of boron incorporated into brucite

Many studies have indicated that only $B(OH)_4^-$ is incorporated preferentially into corals marine carbonates (Vengosh et al., 1991; Hemming and Hanson, 1992; Hemming et al., 1995; Spivack et al., 1993; Sanyal et al., 1996, 2000). Under this circumstance, all the $\delta^{11}B$ values of carbonates are considered to be paralleled with the theoretical $\delta^{11}B_{sw3}$ and are lower than that of the parent seawater; $\alpha_{carb-sw}$ between carbonates and seawater are lower than 1 and increase with pH. When boron is adsorbed by oxides or clay minerals, the adsorption ability of $B(OH)_4^-$ is much stronger than that of $B(OH)_3$. The $B(OH)_4^-$ is also incorporated preferentially into oxides or clay minerals, causing the enrichment of ^{10}B in oxides or clay minerals. Our results show that $\delta^{11}B_d$ is higher than $\delta^{11}B_{isw}$ and parallels neither with $\delta^{11}B_{isw4}$ nor with $\delta^{11}B_{isw3}$, but changes from decrease to increase with an inflexion at pH 12 (Fig. 3b). This indicates that both $B(OH)_4^-$ and $B(OH)_3$ are incorporated into brucite, and the latter is incorporated into brucite preferentially. Boron incorporation into brucite may be controlled by two processes: chemical reaction of $B(OH)_3$ with brucite and $B(OH)_4^-$ adsorption onto brucite. The simultaneous occurrence of these two processes decides the boron concentration and isotopic fractionation of brucite. The mechanisms of boron incorporated into brucite are distinct from those of carbonates and oxides or clay minerals.

5 Judgment method for the existence of brucite in corals and its potentialapplication in δ^{11}B-pH proxy and Mg/Ca-SST proxy

The incorporation of Mg into coral skeleton was controlled by varying factors. Fallon et al. (1999) suggested that variations in Mg data in *Porites* could be a result, not of temperature changes but of possible micro-scale heterogeneities. Mitsuguchi et al. (2003) reported an Mg/Ca offset and believed to be a result of a biological/metabolic effect. Weinbauer et al. (2000) studied the potential use of Mg as an environmental indicator in the coral *Corallium rubrum*, founding

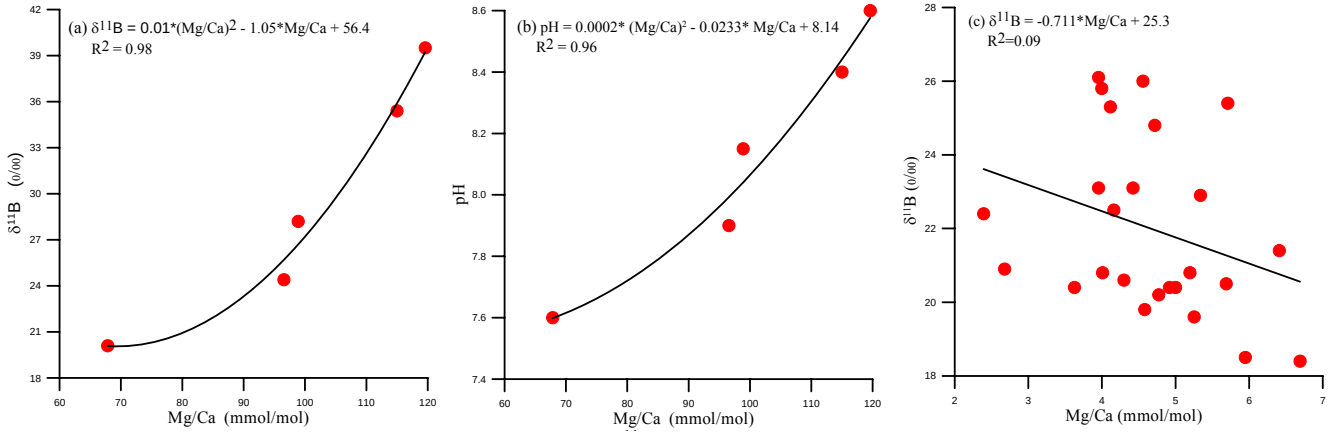

Fig. 9. Relationship **(a)** between Mg/Ca and δ^{11}B in inorganic calcite, **(b)** between Mg/Ca and seawater pH (Xiao et al., 2006a), and (c) between Mg/Ca and δ^{11}B in corals in Sanya Bay (Xiao et al., 2006b). The Mg/Ca was positive with δ^{11}B in inorganic calcite and increased with the seawater pH.

that overall Mg incorporation was controlled by temperature. But the physiology within the coral colony may account for differing amounts of Mg among skeletal structures. A recent study (Nothdurft et al., 2005) showed that brucite exists in a wide range of common reef-building coral in Great Barrier Reef and Florida. Elevated Mg concentrations in modern *scleractinians* may promote the formation of high-Mg calcite cements, as observed in Holocene corals from Heron Reef (Nothdurft et al., 2005), and then cause the deviation from the normal SST-Mg/Ca curves. Samples of brucite-bearing corals could be responsible for anomalies Mg/Ca vs. SST plots in corals (Nothdurft et al., 2005). Thus, corals should be cautiously used, especially brucite-bearing corals, to reconstruct SST. If the variation of Mg/Ca can not be defined exactly, the Mg/Ca-SST proxy would become more complex. In addition, the influence of brucite in corals on the δ^{11}B-pH proxy is more severe. Because one of the essential hypotheses for the δ^{11}B-pH proxy is that only the $B(OH)_4^-$ incorporated into corals, that is ^{10}B incorporated into corals preferentially (Vengosh et al., 1991; Hemming and Hanson, 1992; Sanyal et al., 1996). Under this circumstance, the boron isotope fractionation factor between coral and seawater is less than one. When brucite deposited from seawater, ^{11}B enriched into brucite, the fractionation factor between brucite and seawater is greater than one, which is entirely different from those into corals (Fig. 3). The occurrence of brucite in coral can change the isotopic composition of boron in coral due to the heavier $B(OH)_3$ species incorporated preferentially into brucite and the deviant high boron isotopic composition of corals may associate with the occurrence of brucite. If the brucite-bearing corals were used in δ^{11}B-pH proxy, the measured δ^{11}B of coral and the calculated pH will be higher than the normal value. Rollion-Bard et al. (2011) suggested that careful sampling is necessary before performing boron isotopic measurements in deep-sea corals. So the existence of brucite in corals can negatively influence the Mg/Ca-SST proxy and the δ^{11}B-pH proxy. How to judge the variation of δ^{11}B and Mg/Ca in corals caused by brucite is important for the δ^{11}B-pH proxy and the Mg/Ca-SST proxy. Abnormal boron isotope fractionation ($\alpha_{carb/sw} > 1$) was observed in an inorganic calcite precipitation experiment carried out by Xiao et al. (2006a). They reasoned that the simultaneous deposition of brucite with inorganic calcite was the main reason for this observation. Under this circumstance, the δ^{11}B and Mg/Ca of inorganic calcite have a good positive relationship with correlation coefficients of 0.98 (Fig. 9a). In addition, Mg/Ca was independent of SST, but increased with seawater pH (Fig. 9b), indicating the high Mg/Ca ratio and δ^{11}B were due to the increasing brucite deposition as seawater pH increases. These observations provide a new method for differentiating the existence of brucite in corals. The weak negative relationship between the δ^{11}B and Mg/Ca in corals in Sanya Bay (Fig. 9b) indicated there is no brucite existing in corals in this area. Thus, the relationship between δ^{11}B and Mg/Ca in corals can be used to judge the existence of brucite in corals, which should provide a reliable method for better use of δ^{11}B and Mg/Ca in corals to reconstruct paleo-marine environment.

6 Conclusions

Based on the above experimental results, the following conclusions can be drawn:

1. Boron concentration of deposited brucite and partition coefficient K_d between deposited brucite and resultant seawater is controlled by the pH of solution. The incorporation capacity of boron into brucite is much stronger than that into oxides and clay minerals.

2. All the $\delta^{11}B_d$ values are higher than $\delta^{11}B_{fsw}$ and all the fractionation factors α_{d-fsw} are higher than 1, indicating the preferential incorporation of H_3BO_3 into $Mg(OH)_2$. The mechanism of boron incorporated into brucite is distinct from that of carbonates deposition.

3. During deposition of brucite, both H_3BO_3 and $B(OH)_4^-$ incorporated into brucite. The simultaneous occurrence of boron adsorption onto brucite and the precipitation reaction of H_3BO_3 with brucite decide the boron concentration and isotopic fractionation of the resulting brucite.

4. The existence of brucite in corals can affected the $\delta^{11}B$ and Mg/Ca in corals and influences the Mg/Ca-SST proxy and $\delta^{11}B$-pH proxy negatively. The relationship between $\delta^{11}B$ and Mg/Ca in corals can be used to judge the existence of brucite in corals, which should provide a reliable method for better using of δ^{11}11B and Mg/Ca in corals for the reconstruction of the paleo-marine environment.

Acknowledgements. This project was supported by the National Natural Science Foundation of China (Grant No. 40573013, 40776071 and 41003012), and by the innovation fund of the Institute of Earth Environment, Chinese Academy of Sciences (Grant No. 0951071293). The authors thank Mr. Guohong Gong, Bo Yang and Hua Ge for conducting the XRD and SEM analyses. We also thank the editor Christine Hatté and two anonymous reviewers for their constructive comments and assistance in improving the manuscript.

Edited by: C. Hatté

References

Allison, N., Finch, A. A., and EIMF.: δ^{11}B, Sr, Mg and B in a modern *Porites* coral: the relationship between calcification site pH and skeletal chemistry, Geochim. Cosmochim. Acta., 74, 1790–1800, 2010.

Catanzaro, E. J., Champion, C. E., Garner, E. L., Marinenko, G., Sappenfield, K. M., and Shield, W. R.: Boric acid: Isotopic and assay standard reference materials, US Natl. Bur. Stand. Spec. Publ., 260, 17–70, 1970.

de la Fuente, M. and Muñoz, E.: Boron removal by adsorption with magnesium oxide, Sep. Purif. Technol., 48, 36–44, 2006.

Dickson, A. G.: Thermodynamics of the dissociation of boric acid in synthetic seawater from 273.15 to 318.15 K, Deep-Sea Res. Pt. A., 37, 755–766, 1990.

Douville, E., Paterne, M., Cabioch, G., Louvat, P., Gaillardet, J., Juillet-Leclerc, A., and Ayliffe, L.: Abrupt sea surface pH change at the end of the Younger Dryas in the central subequatorial Pacific inferred from boron isotope abundance in corals (*Porites*), Biogeosciences, 7, 2445–2459, doi:10.5194/bg-7-2445-2010, 2010.

Fallon, S. J., McCulloch, M. T., Woesik, R., and Sinclair, D. J.: Corals at their latitudinal limits: Laser ablation trace element systematics in *Porites* from Shirigai Bay, Japan, Earth Planet. Sc. Lett., 172, 221–238, 1999.

Foster, G. L., Pogge von Strandmann, P. A. E., and Rae, J. W. B.: Boron and magnesium isotopic composition of seawater, Geochem. Geophy. Geosy.,11, Q08015, doi:10.1029/2010GC003201, 2010.

Gaillardet, J. and Allègre, C. J.: Boron isotopic compositions of coral: Seawater or diagenesis record?, Earth Planet. Sc. Lett., 136, 665–676, 1995.

Garcia-Soto, M. D. D. and Camacho, E. M.: Boron removal by means of adsorption with magnesium oxide, Sep. Sci. Technol., 48, 36–44, 2006.

Goldberg, S. and Glaubig, R. A.: Boron adsorption on aluminum and iron oxide minerals, Soil Sci. Soc. Am. J., 49, 1374–1379, 1985.

Goldberg, S. and Glaubig, R. A.: Boron adsorption and silicon release by the clay minerals kaolinite, montmorillonite, and illite, Soil Sci. Soc. Am. J., 50, 1442–1446, 1986.

Hemming, N. G. and Hanson, G. N.: Boron isotopic composition and concentration in modern marine carbonates, Geochim. Cosmochim. Acta., 56, 537–543, 1992.

Hemming, N. G., Reeder, R. J., and Hanson, G. N.: Mineral-fluid partitioning and isotopic fractionation of boron in synthetic calcium carbonate, Geochim. Cosmochim. Acta., 59, 371–379, 1995.

Ingri, N., LagerstrÖm, G., Frydman, M., and Sillën, L. G.: Equilibrium studies of polyanions II polyborates in $NaClO_4$ medium, Acta Chem. Scand., 11, 1034–1058, 1957.

Keren, R., Gast, R. G., and Bar-Yosef, B.: pH-dependent boron adsorption by Na-montmorillonite, Soil Sci. Soc. Am. J., 45, 45–48, 1981.

Keren, R. and Gast, R. G.: pH-dependent boron adsorption by montmorillonite hydroxy-aluminium complexes, Soil Sci. Soc. Am. J., 47, 1116–1121, 1983.

Kingston, F. J., Posner, A. M., and Quirk, J. P.: Anion adsorption by goethite and gibbsite: 1. The role of the proton in determining adsorption envelopes, J. Soil Sci., 23, 177–192, 1972.

Klochko, K., Kaufman, A. J., Yao, W., Byrne, R. H., and Tossell, J. A.: Experimental measurements of boron isotope fractionation in seawater, Earth Planet. Sc. Lett., 248, 261–270, 2006.

Klochko, K., Cody, G. D., Tossell, J. A., Dera, P., and Kaufman, A. J.: Re-evaluating boron speciation in biogenic calcite and aragonite using ^{11}B MAS NMR, Geochim. Cosmochim. Acta., 73, 1890–1900, 2009.

Lemarchand, E., Schott, J., and Gaillardet, J.: Boron isotope fractionation related to boron sorption on humic acid and the structure of surface complexes formed, Geochim. Cosmochim. Acta., 69, 3519–3533, 2005.

Lemarchand, E., Schott, J., and Gaillardet, J.: How surface complexes impact boron isotope fractionation: Evidence from Fe and Me oxide sorption experiments, Earth Planet. Sc. Lett., 260, 277–296, 2007.

Liu, Y., Liu, W. G., Peng, Z. C., Xiao, Y. K., Wei, G. J., Sun, W. D., He, J. F., Liu, G. J., and Chou, C. L.: Instability of seawater pH in the South China Sea during the mid-late Holocene: Evidence from boron isotopic composition of corals, Geochim. Cosmochim. Acta, 73, 1264–1272, 2009.

Liu, Y. S., Li, F. Q., and Wu, Z. M.: Study on adsorption of boron on magnesium hydroxide in brine, J. Salt Lake Res., 12, 45–48, 2004.

Mitsuguchi, T., Matsumoto, E., and Uchida, T.: Mg/Ca and Sr/Ca ratios of Porites coral skeleton: Evaluation of the effect of skeletal growth rate, Coral Reefs, 22, 381–388, 2003.

Mitsuguchi, T., Dang, P. X., Kitagawa, H., Uchida, T., and Shibata, Y.: Coral Sr/Ca and Mg/Ca records in Con Dao Island off the Mekong Delta: Assessment of their potential for monitoring ENSO and East Asian monsoon, Global Planet. Change, 63, 341–352, 2008.

Nothdurft, L. D., Webb, G. E., Buster, N. A., Holmes, C. W., Sorauf, J. E., and Kloprogge, J. T.: Brucite microbialites in living coral skeletons: Indicators of extreme microevironments in shallow-marine settings, Geology, 33, 169–172, 2005.

Palmer, M. R., Spivack, A. J., and Edmond, J. M.: Temperature and pH controls over isotopic fractionation during absorption of boron on marine clay, Geochim. Cosmochim. Acta., 51, 2319–2323, 1987.

Pelejero, C., Calvo, E., McCullogh, M. T., Marshall, J. F., Gagan, M. K., Lough, J. M., and Opdyke, B. N.: Preindustrial to Modern interdecadal variability in Coral Reef pH, Science, 309, 2204–2207, 2005.

Rodionov, A. I., Voitova, O. M., and Romanov, N. Y.: The current state of the problem of the elimination of boron from waste waters, Russ. Chem. Rev., 60, 1271–1279, 1991.

Rollion-Bard, C., Blamart, D., Trebosc, J., Tricot, G., Mussi, A., and Cuif, J. P.: Boron isotopes as pH proxy: A new look at boron speciation in deep-sea corals using ^{11}B MAS NMR and EELS, Geochim. Cosmochim. Acta, 75, 1003–1012, 2011.

Sanchez-Valle, C., Reynard, B., Daniel, I., Lecuyer, C., Martinez, I., and Chervin, J. C.: Boron isotopic fractionation between minerals and fluids: New insights from in situ high pressure-high temperature vibrational spectroscopic data, Geochim. Cosmochim. Acta, 69, 4301–4313, 2005.

Sanyal, A., Hemming, N. G., Broecker, W. S., Lea, D. W., Spero, H. J., and Hanson G. N.: Oceanic pH control on the boron isotopic composition of foraminifera: evidence from culture experiments, Paleoceanography, 11, 513–517, 1996.

Sanyal, A., Nugent, N., Reeder, R. J., and Bijma, J.: Seawater pH control on the boron isotopic composition of calcite: evidence from inorganic calcite precipitation experiments, Geochim. Cosmochim. Acta, 64, 1551–1555, 2000.

Smith, P. L. and Delong, R. C.: Brucite in modern corals, Geol. Soc. Am., Abstracts with Programs, p.494, 1978.

Spivack, A. J., You, C. F., and Smith, H. J.: Foraminiferal boron isotopic ratios as a proxy for surface ocean pH over the past 21 Myr, Nature, 363, 149–151, 1993.

Vengosh, A., Kolodny, Y., Starinsky, A., Chivas, A. R., and McCulloch, M. T.: Coprecipitation and isotopic fractionation of boron in modern biogenic carbonates, Geochim. Cosmochim. Acta, 55, 2901–2910, 1991.

Wang, Q. Z., Xiao, Y. K., Wang, Y. H., Zhang, C. G., and Wei, H. Z.: Boron separation by the two-step ion-exchange for the isotopic measurement of boron, Chin. J. Chem., 20, 45–50, 2002.

Watanabe, T., Winter A., and Oba, T.: Seasonal changes in sea surface temperature and salinity during the Little Ice Age in the Caribbean Sea deduced from Mg/Ca and $^{18}O/^{16}O$ ratios in corals, Mar. Geol., 173, 21–35, 2001.

Wei, G. J., McCulloch, M. T., Mortimer, G., Deng, W. F., and Xie, L. H.: Evidence for ocean acidification in the Great Barrier Reef of Australia, Geochim. Cosmochim. Acta, 73, 2332–2346, 2009.

Weinbauer, M. G., Brandstätter, F., and Vilimirov, B.: On the potential use of magnesium and strontium concentrations as ecological indicators in the calcite skeleton of the red coral (*Corallium rubrum*), Mar. Boil., 137, 801–809, 2000.

Xiao, Y. K., Beary, E. S., and Fassett, J. D.: An improved method for the high precision isotopic measurement of boron by thermal ionization mass spectrometry, Int. J. Mass Spectrom. Ion Proc., 85, 203–213, 1988.

Xiao, Y. K., Liao, B. Y., Liu, W. G., Xiao, Y., and Swihart, G. H.: Ion ex-change extraction of boron from aqueous fluids by Amberlite IRA 743 resin, Chin. J. Chem., 21, 1073–1079, 2003.

Xiao, Y. K., Li, S. Z., Wei, H. Z., Sun, A. D., Zhou, W. J., and Liu, W. G.: An unusual isotopic fractionation of boron in synthetic calcium carbonate precipitated from seawater and saline water, Sci. China Ser. B., 36, 263–272, 2006a.

Xiao, Y. K., Shirodkar, P. V., Zhang, C. G., Wei, H. Z., Liu, W. G., and Zhou, W. J.: Isotopic fractionation of boron in growing corals and its palaeoenvironmental implication, Curr. Sci., 90, 414–420, 2006b.

Xu, L. and Ye, D. H.: Study on electrical property of $Mg(OH)_2$ after boron adsorption, Mar. Sci., 37, 12–13, 1997.

Yuan, J. J., Cui, R., and Zhang, Y.: Study on the adsorption of magnesium hydroxide to boron in seawater and the removal of boron in brine, J. Salt Chem. Ind., 36, 1–6, 2006.

Zeebe, R. E.: Stable boron isotope fractionation between dissolved $B(OH)_3$ and $B(OH)_4^-$, Geochim. Cosmochim. Acta, 69, 2753–2766, 2005.